

Dropwise condensation on superhydrophobic surfaces with two-tier roughness

Chuan-Hua Chen,^{a)} Qingjun Cai, Chialun Tsai, and Chung-Lung Chen
Teledyne Scientific Company, 1049 Camino Dos Rios, Thousand Oaks, California 91360

Guangyong Xiong, Ying Yu, and Zhifeng Ren
Department of Physics, Boston College, Chestnut Hill, Massachusetts 02467

(Received 5 December 2006; accepted 24 March 2007; published online 24 April 2007)

Dropwise condensation can enhance heat transfer by an order of magnitude compared to film condensation. Superhydrophobicity appears ideal to promote continued dropwise condensation which requires rapid removal of condensate drops; however, such promotion has not been reported on engineered surfaces. This letter reports continuous dropwise condensation on a superhydrophobic surface with short carbon nanotubes deposited on micromachined posts, a two-tier texture mimicking lotus leaves. On such micro-/nanostructured surfaces, the condensate drops prefer the Cassie state which is thermodynamically more stable than the Wenzel state. With a hexadecanethiol coating, superhydrophobicity is retained during and after condensation and rapid drop removal is enabled. © 2007 American Institute of Physics. [DOI: 10.1063/1.2731434]

Dropwise condensation on a hydrophobic surface has been known to enhance heat transfer by approximately an order of magnitude compared to film condensation on a hydrophilic one.^{1,2} Rapid removal of large condensate drops is essential to continuous dropwise condensation, for which superhydrophobic surfaces appear to be an ideal solution. On a roughened hydrophobic surface, a liquid drop can exhibit either the Cassie state where the drop sits on the air-filled textures³ or the Wenzel state where the drop wets cavities of the textures.⁴ The apparent contact angle of a roughened hydrophobic surface is enhanced in both the Cassie and Wenzel states; however, the Cassie state is the preferred superhydrophobic state in which a drop has a much smaller contact angle hysteresis and therefore a higher mobility.⁵ To date, none of the reported condensation on engineered superhydrophobic surfaces exhibits a sustained Cassie state; instead, the condensate drops partially or fully penetrate into the cavities over the course of condensation.^{5–8} Further, laboratory condensation on superhydrophobic lotus leaves shows similar penetration behavior and condensate drops tend to stick to the cooled lotus leaves.^{9,10}

Here, we report continuous dropwise condensation on a two-tier texture which retains superhydrophobicity during and after condensation. The two-tier texture, mimicking that on the surface of lotus leaves,¹¹ was prepared by depositing carbon nanotubes (CNTs) on micromachined pillars (Fig. 1). On a $2 \times 2 \times 0.1$ cm³ silicon (Si) substrate, squarely positioned pillars were etched at the center (1.5×1.5 cm²) by deep reactive ion etching. The etched Si substrates were coated with a thin layer of chromium (Cr, 100 nm) and then nickel (Ni, 20 nm) as catalyst, and CNTs were grown by plasma enhanced chemical vapor deposition.¹² The substrate was then hydrophobized either by a 10 nm layer of parylene C coating or by a 10 nm layer of gold coated with a monolayer of 1-hexadecanethiol (Fluka 52270).¹³ For comparison purposes, some one-tier microtextures were prepared by skipping the step of CNT deposition (i.e., only Si micro-

pillars) but were otherwise processed in the same manner. In addition, the edges of the two-tier substrates (where there were only CNT nanopillars) were used as examples of one-tier nanotextures. The dimensions of these textures (Table I) were measured by scanning electron microscopy (SEM) at a tilt angle of 30° (Philips XL30). The dry substrate was held (assisted by a thin film of water) on a copper plate cooled by a recirculating chiller. The plate surface in contact with the substrate was maintained at 5 °C, while the ambient air was at 19 °C with a relative humidity of 74%, corresponding to a dew point of 14 °C. The condensation of water vapor onto the substrate was visualized by an optical microscope (Nikon LV150) with a 10× lens (numerical aperture=0.3) and a charge-coupled device camera (SensiCam SVGA). Images were captured at 1 frame per second (fps) with an exposure time of 10 ms.

The carbon nanotubes used here as the secondary roughness have two noteworthy features compared to other superhydrophobic surfaces incorporating CNTs (see, for example, Refs. 14–17). (i) The Cr–Ni catalyst layer was not removed; therefore, the carbon nanotubes with catalyst “caps” worked

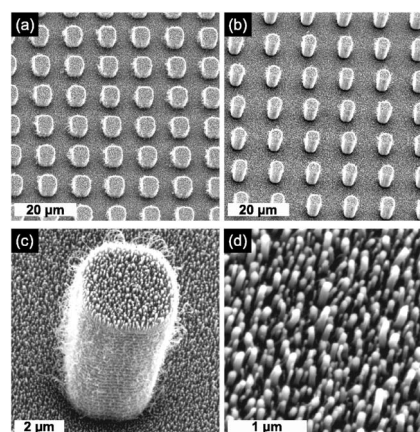


FIG. 1. Two-tier textures: micropillars are etched in silicon, and CNT nanopillars are subsequently deposited. (a) Structure A_{mn} , (b) structure B_{mn} , (c) micropillar of B_{mn} , (d) CNT nanopillars (A_n, B_n).

^{a)}Electronic mail: chchen@teledyne.com

TABLE I. Parameters of microtextures (A_m, B_m), nanotextures (A_n, B_n), and two-tier textures (A_{mn}, B_{mn}). Physical dimensions of pillars: width w (cross section approximated as square), center-to-center separation s , and height h . Structural properties of rough surface: solid fraction f and surface roughness r , both determining a critical contact angle θ_c .

Structure	w (μm)	s (μm)	h (μm)	f	r	θ_c
A_m	4.9	11.2	5.2	0.19	1.8	120°
B_m	3.7	12.0	8.0	0.095	1.8	122°
A_n, B_n^a	0.06	0.12	0.4	0.25	7.7	96°
A_{mn}	0.048	14	94°
B_{mn}	0.024	14	94°

^aThe CNT pillars on both microstructures were processed under the same condition: $w_n=60\pm 40$ nm, $h_n=400\pm 100$ nm, and $s_n\approx 120\pm 80$ nm. The surface coverage of CNT pillars (f) was also independently measured as $(25\pm 5)\%$ by image processing.

like solid nanopillars as far as surface wettability was concerned. (ii) These nanopillars had an average length of 400 nm, much shorter compared to micrometric carbon nanotubes previously used. The shorter nanopillars are closer to the 100 nm scale secondary roughness on lotus leaves.¹¹ Further, shorter nanotubes are more rigid and prevent nanotube bundling due to capillary forces,^{14,15} as shown by SEM images in Fig. 1 which were all taken after repeated condensation experiments.

A liquid drop on a roughened surface can exhibit either Cassie or Wenzel state, which is demarcated by a critical contact angle θ_c . The Cassie state is thermodynamically more stable when the physical contact angle θ_p (i.e., on a smooth surface) is greater than the critical one,¹⁸

$$\theta_p > \theta_c, \text{ with } \cos \theta_c = -\frac{1-f}{r-f}. \quad (1)$$

In lack of a generally accepted definition of θ_p , we use static contact angle to approximate θ_p .¹⁹ On a one-tier texture of squarely positioned square posts with width w , center-to-center separation s , and height h , $f=w^2/s^2 < 1$ is the fraction of solid surface in contact with liquid in the heterogeneous Cassie state, and $r=(s^2+4wh)/s^2 > 1$ is the roughness ratio of total surface area in contact with liquid over the projected area in the penetrated Wenzel state.¹⁸ According to Eq. (1), there are two routes to a stable Cassie state: (i) Decreasing the critical contact angle using a texture with lower f and higher r . A two-tier design suits this purpose as $f_{mn}=f_m f_n$ and $r_{mn}=r_m r_n$, where subscripts m denotes microtexture, n nanotexture, and mn two-tier texture. (ii) Increasing the physical contact angle, e.g., from parylene coating ($\theta_p=91^\circ\pm 4^\circ$ with advancing and receding contact angles $\theta_a/\theta_r=98^\circ/59^\circ$) to hexadecanethiol coating ($\theta_p=101^\circ\pm 4^\circ$ with $\theta_a/\theta_r=116^\circ/87^\circ$).¹⁹

The importance of the two-tier design is shown in Fig. 2 by the coalescence of condensate drops on different texture designs with the same parylene coating. On a one-tier texture with only micropillars [Figs. 2(a) and 2(b)], the condensate drops penetrated into the interstitial cavities, an observation consistent with the literature on similar micromachined structures.^{7,8} On another one-tier texture with only nanopillars [Figs. 2(c) and 2(d)], the condensate drops also appeared to penetrate into the cavities as indicated by the large contact angle hysteresis associated with the irregular drop shape. In contrast, on a two-tier surface with nanopillars on top of micropillars [Figs. 2(e) and 2(f)], the condensate drops

stayed in the Cassie state as indicated by the almost spherical drops [compared to the flattened and irregular drops in Figs. 2(a)–2(d)]. Except for drops with a diameter comparable to the micropillar separation (i.e., $\lesssim 20$ μm), the coalesced drops (some after a series of coalescence) remained in the Cassie state on a two-tier texture during an experimental test span of 1 h.

The difference in condensation behavior resulting from one- and two-tier designs (Table I) can be qualitatively explained by the thermodynamic stability criterion [Eq. (1)]. With a parylene coating, the physical contact angle ($\theta_p=91^\circ\pm 4^\circ$) is below the critical contact angle of both one-tier structures (A_m : $\theta_c=120^\circ$ and A_n : $\theta_c=96^\circ$) but are comparable to a two-tier structure (A_{mn} : $\theta_c=94^\circ$). Therefore, Wenzel state is more stable on the parylene-coated one-tier texture, while Cassie state is more stable on the corresponding two-tier texture. This thermodynamic argument is also supported by the observation that a hexadecanethiol ($\theta_p=101^\circ$) instead of parylene coating made a nanopillar-only texture (A_n) superhydrophobic during and after condensation [see Fig. 4(b), edge of chip with only nanopillars]. Further, similar condensation behaviors were observed on two designs (A_{mn} and B_{mn}) given the same surface coating. These two designs have different solid fractions (f) but the same roughness (r), which supports the asymptotic limit of the thermodynamically based critical angle, $\theta_c \rightarrow -1/r$ for $f \ll 1$ and $r \gg 1$.

Although in the Cassie state, the drops had limited mobility on a parylene-coated two-tier texture, as evident from the nearly stationary drops around the coalescing drops in Figs. 2(e) and 2(f). On a hexadecanethiol-coated two-tier texture, rapid removal of large condensate drops was achieved, as shown by a series of images illustrating the condensation process (Fig. 3). At the initial stage, condensate liquid nucleated both on the top of the micropillars and in the interstitial cavities [Fig. 3(a), at 1 min]. The drops soon started to coalesce and the coalesced drops appeared to be spherical on top of the micropillars, i.e., in the Cassie state [Fig. 3(b), at 2 min]. Similar to the parylene-coated surface, the condensate drops (except those with diameters comparable to the microscale cavities) remained in the Cassie state during condensation. In the continuous process of nucleation, coales-

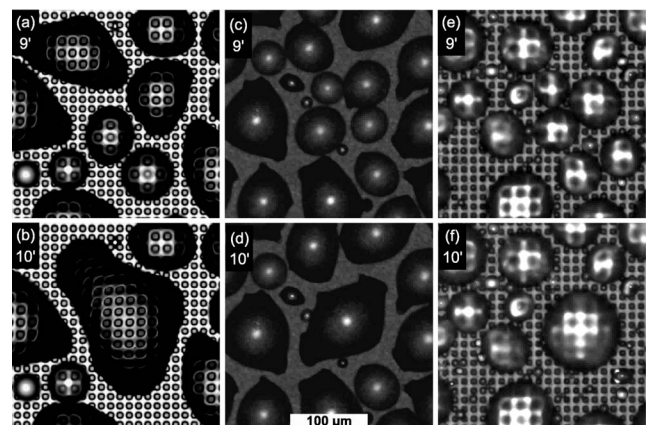


FIG. 2. Coalescence of condensate drops on parylene-coated textures with one- and two-tier roughness. [(a)–(b)] A_m : one tier with only micropillars, [(c)–(d)] A_n : one tier with only nanopillars, and [(e)–(f)] A_{mn} : two-tier roughness. Images are captured at 9 or 10 min after initiation of condensation.

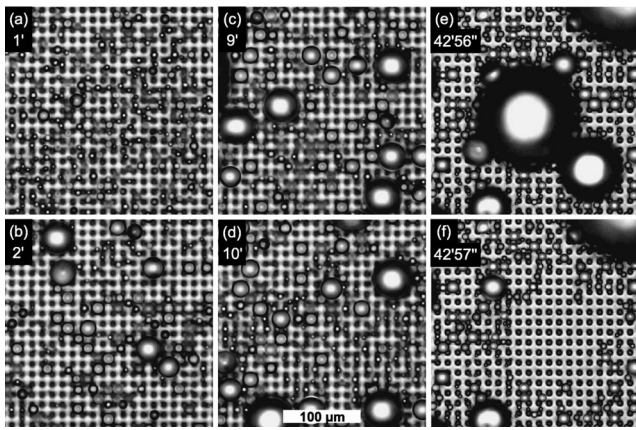


FIG. 3. Condensation process on hexadecanethiol-coated texture with two-tier roughness (B_{mn}). The images are captured over the same area, and time stamps are with respect to the initiation of condensation.

cence, and renucleation, the condensate drops frequently traveled large distances (0.1–10 mm) over short period of time (~ 10 ms) at seemingly random directions.²⁰ The rapid drop motion, usually triggered by coalescence, is apparent by comparing Figs. 3(c) and 3(d) to Figs. 2(e) and 2(f), both taken at 9 and 10 min after condensation started. Compared to the parylene-coated surface, it was no longer possible to track most of the drops on a hexadecanethiol-coated surface after 1 min. Due to the drop coalescence and rapid motion, most condensed liquids were eventually collected into a few large drops, one example being the 120 μm diameter drop shown in Fig. 3(e) (at 42 min 56 s). These large drops retained high mobility, as evident from the disappearance of the example drop within 1 s [Fig. 3(f)].

In addition to maintaining superhydrophobicity during condensation, the hexadecanethiol-coated two-tier surface also retained superhydrophobicity after condensation (Fig. 4). After 1 h of condensation, the substrate temperature was raised to that of the ambient air. The substrate remained on the horizontal microscope stage used for visualization. A hand-held tweezer was used to gently shake the substrate horizontally to induce drop coalescence. The sweeping motion of a large drop left a dry path behind (evident from optical contrast) with small drops absorbed into the large one [Fig. 4(a)]. After a few cycles of horizontal oscillations, nearly all condensate drops were collected into a few large drops, and the hexadecanethiol-coated two-tier surface was almost completely dry [Fig. 4(b)].

The rapid drop removal process on a hexadecanethiol-coated surface (Figs. 3 and 4) was not possible on a parylene-coated surface with the same two-tier design. In-

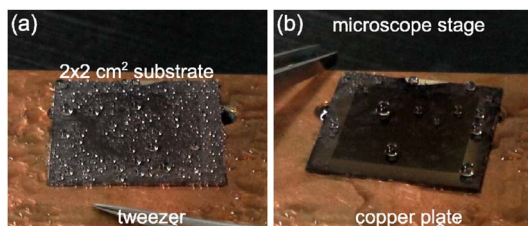


FIG. 4. (Color online) Removal of condensate drops on hexadecanethiol-coated two-tier texture (B_{mn}). (a) After condensation, a tweezer is used to gently shake the substrate horizontally. (b) Most condensate drops are removed after a few cycles of oscillations.

stead, condensate drops tended to stick to the parylene-coated surface and could only be removed by drops of large size or momentum; similar phenomena were observed on condensed lotus leaves.⁹ The improvement over lotus leaf in laboratory condensation reported here is likely to be related to the lower surface energy of the hexadecanethiol coating ($\theta_p = 101^\circ \pm 4^\circ$) compared to the wax coating of lotus leaves ($\theta_p = 74^\circ \pm 9^\circ$).²¹

In summary, we achieved continuous dropwise condensation on a biomimetic two-tier texture with short carbon nanotubes deposited on micromachined pillars. Our hexadecanethiol-coated two-tier textures appeared to surpass lotus leaves in terms of retaining superhydrophobicity during and after laboratory condensation. The thermodynamic criterion for stable Cassie state was used to guide the geometrical design and surface treatment and can also qualitatively explain several experimental observations. However, much work is needed to quantitatively understand the dynamic condensation process down to the nanoscale, both in laboratory and in nature. A clear understanding of superhydrophobic condensation experimentally reported here not only has applications in two-phase heat transfer but also impacts the engineering of robust superhydrophobic materials in general.

This work was supported by the Office of Naval Research under Contract No. N00014-06-C-0015 with M. Spector as program manager. The authors thank W. Pan, R. Chen, M. Calabrese, and D. Strauss for technical assistances and D. Beysens for sharing an unpublished manuscript.

¹E. Schmidt, W. Schurig, and W. Sellschopp, *Tech. Mech. Thermodyn. (Forsch. Ing. Wes.)* **1**, 53 (1930).

²J. W. Rose, *Proc. Inst. Mech. Eng., Part A* **216**, 115 (2002).

³A. B. D. Cassie and S. Baxter, *Trans. Faraday Soc.* **40**, 546 (1944).

⁴R. N. Wenzel, *Ind. Eng. Chem.* **28**, 988 (1936).

⁵A. Lafuma and D. Quere, *Nat. Mater.* **2**, 457 (2003).

⁶R. D. Narhe and D. A. Beysens, *Phys. Rev. Lett.* **93**, 076103 (2004).

⁷R. D. Narhe and D. A. Beysens, *Europhys. Lett.* **75**, 98 (2006).

⁸K. A. Wier and T. J. McCarthy, *Langmuir* **22**, 2433 (2006).

⁹Y. T. Cheng and D. E. Rodak, *Appl. Phys. Lett.* **86**, 144101 (2005).

¹⁰Y. T. Cheng, D. E. Rodak, A. Angelopoulos, and T. Gacek, *Appl. Phys. Lett.* **87**, 194112 (2005).

¹¹C. Neinhuis and W. Barthlott, *Ann. Bot. (London)* **79**, 667 (1997).

¹²Z. F. Ren, Z. P. Huang, J. W. Xu, J. H. Wang, P. Bush, M. P. Siegal, and P. N. Provencio, *Science* **282**, 1105 (1998).

¹³Parylene C was conformally coated using a parylene deposition system (Specialty Coating Sys., PDS2010) and a dichloro-diparaxylylene dimer. Hexadecanethiol monolayer was self-assembled by dipping the gold-coated substrate in 1 mM ethanol solution of 1-hexadecanethiol for 90 s, followed by ethanol washing and air drying.

¹⁴K. K. S. Lau, J. Bico, K. B. K. Teo, M. Chhowalla, G. A. J. Amarantunga, W. I. Milne, G. H. McKinley, and K. K. Gleason, *Nano Lett.* **3**, 1701 (2003).

¹⁵C. Journet, S. Moulinet, C. Ybert, S. T. Purcell, and L. Bocquet, *Europhys. Lett.* **71**, 104 (2005).

¹⁶L. Zhu, Y. Xiu, J. Xu, P. A. Tamirisa, D. W. Hess, and C.-P. Wong, *Langmuir* **21**, 11208 (2005).

¹⁷H. Liu, J. Zhai, and L. Jiang, *Soft Matter* **2**, 811 (2006).

¹⁸D. Quere, *Rep. Prog. Phys.* **68**, 2495 (2005).

¹⁹The static contact angle was measured on a 0.5 μl sessile drop immediately after the pipetted drop reached a quasiequilibrium shape on a horizontal surface. Advancing and receding contact angles were measured by incrementally increasing the size of a sessile drop on a surface slanted at 30° to the point of marginal motion.

²⁰High-speed imaging at 1000 fps revealed a rapid drop motion at a speed of order 10 cm/s and accelerations up to 10g. A detailed analysis will be presented elsewhere.

²¹Y. T. Cheng, D. E. Rodak, C. A. Wong, and C. A. Hayden, *Nanotechnology* **17**, 1359 (2006).